CHAPTER 16

Kramers theory

The very fact that a reaction is going on means that [transition states] will never be in exact temperature equilibrium with state A.

Kramers, Physica VII (1940)

Kramers developed an important rate theory that spans a number of dynamical regimes [1]. At one extreme, Kramers theory describes a quasi-microcanonical dynamics where the rate is limited by slow energy transfer processes that cannot activate reactants nor quench activated products. At the other extreme, Kramers theory describes processes like nucleation and biomolecular conformational transitions where the dynamics resemble overdamped diffusion over a barrier. An intermediate regime of Kramers theory describes trajectories that cross a critical dividing surface and continue along the reaction coordinate to the product state with few barrier recrossings, almost like the dynamics assumed in transition state theory. These *qualitative* results have been validated in numerous simulations and even in some experiments. In the high friction limit, the Kramers theory is quantitatively correct. In particular, the high friction Kramers theory corroborates Pontryagin's theory of diffusion over barriers [2], classic theories of nucleation [3], theories of polymer relaxation dynamics [4], and some predictions about protein folding rates [5].

However, the Kramers theory has also been criticized because it does not accurately predict transmission coefficients (nor absolute rates) for most chemical reactions [6,7]. The shortcomings of Kramers theory are most severe in the weak-coupling limit, where it ostensibly models unimolecular dissociation reactions in low pressure gases. In this limit, Kramers invokes a steady weak friction that is markedly different from the strong but infrequent collisions that activate real unimolecular decay processes [4,7,8]. Additionally, the inertial Langevin equation at the heart of Kramers theory cannot accurately describe coupling between a slow solvent and rapid motion along a reaction coordinate [9,10].

Nevertheless, Kramers theory does *qualitatively* explain how reaction dynamics and rates depend on coupling between the reaction coordinate and other degrees of freedom. Moreover, Kramers theory inspired several theories that do accurately model reaction dynamics in condensed phases [4,11]. For example, the inertial Langevin equation in the Kramers theory can

be generalized to obtain the Grote-Hynes theory which more accurately predicts transmission coefficients for reactions in solution [9]. Kramers theory has also been generalized to multiple dimensions which extends its domain of validity by explicitly including the dynamics of several slow variables [12,13].

Kramers theory continues to evolve, but experiments that test its predictions about solvent viscosity and chemical reaction rates in solution remain difficult [7,14,15]. Efforts to modify the solvent viscosity invariably also make small changes in solvation free energies and therefore in the free energy barrier. Simulations and particularly rare events methods, where dynamics and thermodynamics can be separately manipulated, provide one of the best arenas to test theories of reaction dynamics in the condensed phase. Additionally, there are continuing efforts to forge a better understanding of the abstract parameters in the Kramers theory and thereby to enable more easily tested predictions [16–20].

16.1 Intermediate and high friction

The starting point in Kramers theory is the inertial Langevin equation [1,21]. The inertial Langevin equation and its properties were discussed in Chapter 15, but let us briefly recap the main points. The inertial Langevin equation is

$$m\ddot{q} = -\frac{\partial V}{\partial q} - m\gamma\dot{q} + R(t) \tag{16.1.1}$$

Here q represents a reaction coordinate, m is the reduced mass/inertia for the reaction coordinate, γ is the friction, and $V(q)$ is a potential of mean force (PMF).[1] $R(t)$ is a random force that models the effects of bath degrees of freedom on the reaction coordinate. The random force along coordinate q has zero mean, $\langle R(t)\rangle = 0$, and a delta correlated variance as required by the fluctuation dissipation theorem [21]: $\langle R(t)R(0)\rangle = 2m\gamma k_B T\delta[t]$.

In principle, the Langevin equation can be constructed from molecular simulations. For example, the effective mass associated with a coordinate q can be obtained from equipartition: $m\langle\dot{q}^2\rangle = k_B T$. The effective friction can also be computed using clamped simulations as described in Chapter 17. The PMF can be computed using umbrella sampling or other methods for computing free energies. In real systems, these calculations are complicated because the effective mass m, the friction γ, and of course $V(q)$ are functions of the location along q. Let us postpone computational procedures until the next chapter. Here we follow Kramers in considering a constant mass m, a constant friction γ, and an idealized parabolic barrier model for the PMF.

[1] Systems described by Kramers theory span the condensed phase (where we might obtain $-\partial V/\partial q$ by differentiating a free energy profile $F(q)$) to a nearly isolated degree of freedom (where we might obtain $-\partial V/\partial q$ by differentiating the Born-Oppenheimer potential).

First, note that the inertial Langevin equation (16.1.1) can be rewritten as a system of first order equations for the position q and velocity v along the reaction coordinate. The pair of equations is $dq/dt = v$ and $m\,dv/dt = -\partial V/\partial q - m\gamma v + R(t)$. These equations can be converted to a special Klein-Kramers type Fokker-Planck equation for the probability density $\rho(q, v, t)$ [21, 22]:

$$\frac{\partial \rho}{\partial t} = \left\{ -v\frac{\partial}{\partial q} + \gamma \frac{\partial}{\partial v}\left(v + \frac{k_B T}{m}\frac{\partial}{\partial v}\right) + \frac{1}{m}\frac{\partial V}{\partial q}\frac{\partial}{\partial v}\right\}\rho \tag{16.1.2}$$

Kramers' theory models the barrier as a parabolic potential

$$V(q) = V_{\ddagger} - \frac{1}{2}m\omega_{\ddagger}^2(q - q_{\ddagger})^2 \tag{16.1.3}$$

Let us assume for convenience that the value of $q_{\ddagger} = 0$, i.e. that transition states are located at the origin on the q-axis. We can always shift q by $q_{\ddagger}$ to make the origin coincide with the transition state. Later in our discussion we will make another harmonic approximation to the PMF in the reactant minimum. Kramers theory assumes nothing about the product state except that it should irreversibly absorb reactive trajectories. The PMF and the two harmonic approximations are shown in Figure 16.1.1.

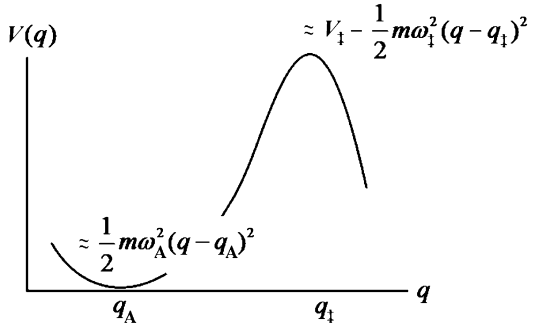

Figure 16.1.1: Harmonic approximations at the reactant minimum (q_A) and barrier top ($q_{\ddagger}$) along a potential energy profile $V(q)$. The bottom of the reactant well is the zero of energy.

Using the parabolic model for $V(q)$ near $q_{\ddagger}$ in the Klein-Kramers equation gives

$$\frac{\partial \rho}{\partial t} = -v\frac{\partial \rho}{\partial q} - \omega_{\ddagger}^2 q\frac{\partial \rho}{\partial v} + \gamma\frac{\partial}{\partial v}(v\rho) + \frac{\gamma k_B T}{m}\frac{\partial^2 \rho}{\partial v^2}$$

TST computes the rate as though the transition states are at equilibrium with the reactants. Instead, Kramers envisioned a steady-state non-equilibrium flux of trajectories over the barrier [1]. If the barrier is large compared to $k_B T$, then an ensemble prepared on the reactant side of the barrier will quickly reach a local equilibrium within the reactant state, perturbed only slightly by a slow leak over the barrier. If we "rescue" each trajectory that escapes to the product side of the barrier and "replace" it on the reactant side, the non-equilibrium system will develop

a steady-state distribution, $\rho_{SS}(q, v)$. Deep within the reactant well, the steady-state distribution will resemble the equilibrium distribution of reactants. Trajectories are always removed from the product side, so ρ_{SS} must approach zero deep within the product basin. For all points between, the non-equilibrium steady-state density must satisfy the equation

$$0 = -v\frac{\partial \rho_{SS}}{\partial q} - \omega_{\ddagger}^2 q\frac{\partial \rho_{SS}}{\partial v} + \gamma\frac{\partial}{\partial v}(v\rho_{SS}) + \frac{\gamma k_B T}{m}\frac{\partial^2 \rho_{SS}}{\partial v^2} \tag{16.1.4}$$

with boundary conditions

$$\rho_{SS}(q, v) \to 0 \quad as \quad q \to \infty \tag{16.1.5}$$

and

$$\rho_{SS}(q, v) \to \rho_{eq}(q, v) \quad as \quad q \to -\infty \tag{16.1.6}$$

We cannot properly normalize $\rho_{eq}(q, v)$ because $exp[-\beta V(q)]$ diverges as $q \to \infty$. Kramers fixed this problem with a crossover function $\xi_{SS}(q, v)$, defined as the ratio of steady-state and equilibrium distributions [1]

$$\xi_{SS}(q, v) \equiv \rho_{SS}(q, v)/\rho_{eq}(q, v) \tag{16.1.7}$$

Substituting the Kramers' crossover definition into equation (16.1.4) for $\rho_{SS}(q, v)$ gives an equation for $\xi_{SS}(q, v)$

$$v\frac{\partial \xi_{SS}}{\partial q} + \omega_{\ddagger}^2 q\frac{\partial \xi_{SS}}{\partial v} + \gamma v\frac{\partial \xi_{SS}}{\partial v} = \frac{\gamma k_B T}{m}\frac{\partial^2 \xi_{SS}}{\partial v^2} \tag{16.1.8}$$

with new asymptotic boundary conditions

$$\xi_{SS}(q, v) \to 0 \quad as \quad q \to \infty$$

and

$$\xi_{SS}(q, v) \to 1 \quad as \quad q \to -\infty$$

The method of characteristics (or an inspired guess [1]) reveals that the dependence on q and v can be collapsed to dependence on a single variable $u = q - av$. To identify the appropriate constant a, use the chain rule to obtain the derivatives $\partial \xi_{SS}/\partial q = \xi'_{SS}(u)$, $\partial \xi_{SS}/\partial v = -a\xi'_{SS}(u)$, and $\partial^2 \xi_{SS}/\partial v^2 = a^2 \xi''_{SS}(u)$. Substitute these into equation (16.1.8) and simplify to obtain

$$-a\omega_{\ddagger}^2\left(q - v\frac{1 - \gamma a}{a\omega_{\ddagger}^2}\right)\xi'_{SS}(u) = \frac{\gamma k_B T}{m}a^2 \xi''_{SS}(u) \tag{16.1.9}$$

The dependence on q and v will collapse to a dependence on the combined variable $u \equiv q–av$ if we can choose a such that equation (16.1.9) contains no independent factors of q and v. Specifically, if we choose a such that the term in parentheses becomes u, we will have eliminated all separate factors of q and v, while still having a linear equation. Therefore we must solve

$$q - v\frac{1-\gamma a}{a\omega_{\ddagger}^2} = q - av$$

to find the appropriate value of a. This equation has two solutions

$$a = -\frac{\gamma}{2\omega_{\ddagger}^2}\left(1 \pm \sqrt{1 + 4\omega_{\ddagger}^2/\gamma^2}\right)$$

For these two choices of a, equation (16.1.9) becomes

$$-\frac{m\omega_{\ddagger}^2}{\gamma k_B T a} u\xi'_{SS}(u) = \xi''_{SS}(u)$$

The general solution is

$$\xi_{SS}(u) = c_2 + c_1 \mathrm{erf}\left[u\sqrt{\frac{m\omega_{\ddagger}^2}{2\gamma k_B T a}}\right]$$

where c_1 and c_2 are integration constants to be determined by the boundary conditions on $\xi_{SS}(u)$. As $q \to \infty$, $u \to \infty$ for any v, and as $q \to -\infty$, $u \to -\infty$ for all v. Therefore, the boundary conditions have become

$$\xi_{SS}(u) \to 0 \quad as \quad u \to \infty$$

and

$$\xi_{SS}(u) \to 1 \quad as \quad u \to -\infty$$

Remembering our convention that $\omega_{\ddagger}^2 > 0$, we must also require $a > 0$ for solutions that do not diverge.[2] Therefore,

$$a = \frac{\gamma}{2\omega_{\ddagger}^2}\left(\sqrt{1 + 4\omega_{\ddagger}^2/\gamma^2} - 1\right)$$

[2] $i\,\mathrm{erf}(i\,u)$ is a real valued function for real u, but it diverges as $u \to \pm\infty$.

From properties of the erf function and the boundary conditions, the limit as $u \to \infty$ gives $\xi_{SS}(u) \to c_2 + c_1$. Therefore, $c_1 = -c_2$. Then as $u \to -\infty$, we find that $\xi_{SS}(u) \to 2c_2$, and therefore to match the left boundary condition $c_2 = 1/2$. Finally, we obtain [1]

$$\xi_{SS}(u) = \frac{1}{2}\text{erfc}\left[\sqrt{\frac{m\omega_{\ddagger}^2}{2\gamma k_B T a}} \cdot u\right] \tag{16.1.10}$$

where $\text{erfc}(x) \equiv 1 - \text{erf}(x)$. The solution for the crossover function is shown in Figure 16.1.2.

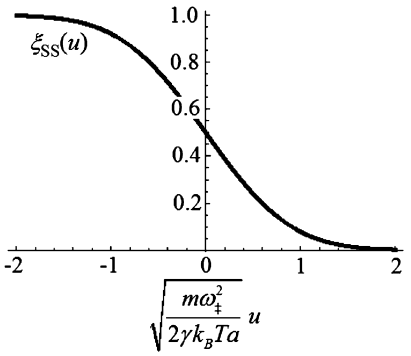

Figure 16.1.2: The Kramers crossover function in terms of the combined variable u.

Now we can use $\xi_{SS}(u)$ to reconstruct the (unnormalized) steady-state distribution

$$\rho_{SS} = \frac{1}{2} exp\left[-\frac{mv^2}{2k_B T} - \frac{1}{k_B T}\left(V_{\ddagger} - \frac{1}{2}m\omega_{\ddagger}^2 q^2\right)\right] \cdot \text{erfc}\left[\sqrt{\frac{m\omega_{\ddagger}^2}{2\gamma k_B T a}}(q - av)\right]$$

With some algebra, $\rho_{SS}(q, v)$, $\rho_{eq}(q, v)$, and $\xi_{SS}(q, v)$ can each be written in terms of dimensionless variables $\underline{q} = m^{1/2}\omega_{\ddagger} q/(k_B T)^{1/2}$ and $\underline{v} = m^{1/2} v/(k_B T)^{1/2}$. This leaves only one parameter, $\gamma/\omega_{\ddagger}$, in the steady-state distribution. In Figures 16.1.3 and 16.1.4 we have made this change of variables and plotted $\xi_{SS}(\underline{q}, \underline{v})$ and $\rho_{SS}(\underline{q}, \underline{v})$.

Several features are noteworthy in these plots. $\rho_{SS}(q, v)$ vanishes as we move toward positive values of q and toward negative values of v. The region where ρ_{SS} vanishes penetrates into the reactant state ($q < 0$) because there are no trajectories returning from the product state. $\rho_{SS}(q, v)$ cannot have support in regions that correspond to trajectories returning from the product state due to the rescue and replace boundary conditions. Additionally, note that isosurfaces of $\rho_{SS}(q, v)$ bend upward as they cross the barrier top because trajectories in the nonequilibrium ensemble tend to accelerate as the barrier is crossed. As friction increases, the velocity at the barrier top becomes increasingly irrelevant. At $\gamma/\omega_{\ddagger} = 4.0$ the steady-state distribution reveals that much of the forward flux is canceled by recrossing, i.e. by trajectories whose velocities are damped out in the barrier region before they fall down into the product state.

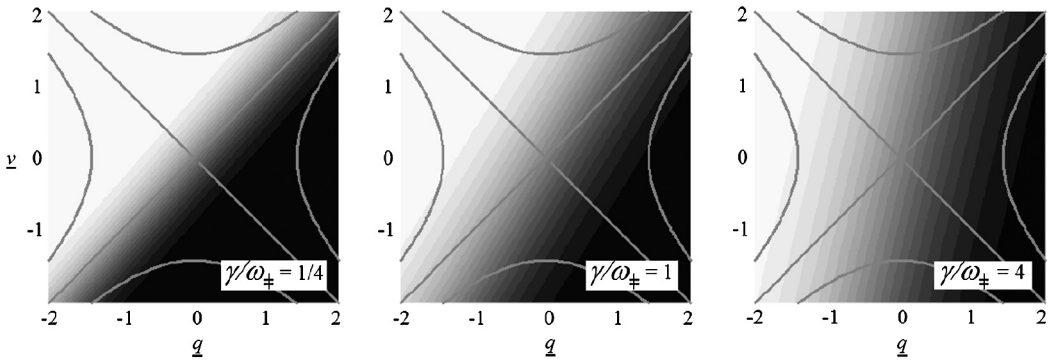

Figure 16.1.3: The contour lines show the total energy as a function of dimensionless position and velocity in the vicinity of the barrier top. The shading shows the Kramers crossover function $\xi_{SS}(\underline{q}, \underline{v})$. The energy and crossover function are shown for three different values of the dimensionless parameter $\gamma/\omega_{\ddagger}$.

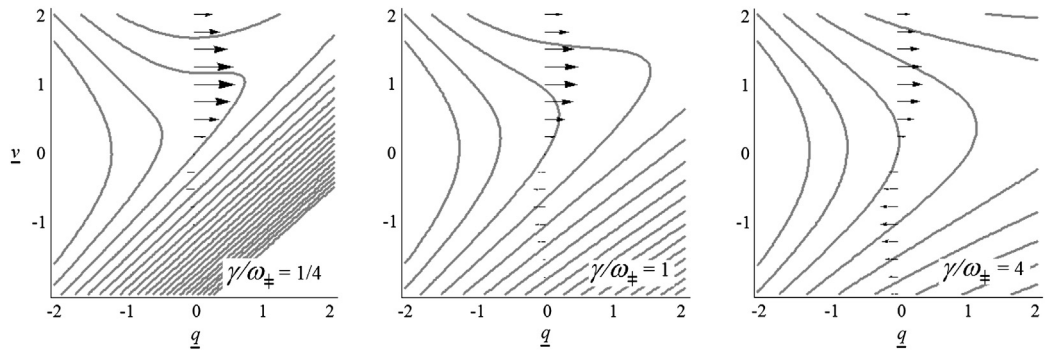

Figure 16.1.4: The contour lines show the steady-state distribution $\rho_{SS}(\underline{q}, \underline{v})$ in the vicinity of the barrier top. The distribution diverges to infinity to the left of the barrier top, and becomes vanishingly small on the product side. The distribution is shown for three different values of the dimensionless parameter $\gamma/\omega_{\ddagger}$. Contours are separated by factors of two in ρ_{SS}. Arrows show the local flux crossing each point on the dividing surface $q = 0$.

To obtain the Kramers rate constant we must normalize $\rho_{SS}(q, v)$ and then compute the flux through a dividing surface [1]. $\rho_{SS}(q, v)$ has negligible support near the barrier top and in the product region. Essentially all support comes from the reactant state where $\rho_{SS}(q, v) \propto \rho_{eq}(q, v)$. Therefore the normalized density is

$$\rho_{SS}(q, v) = \frac{e^{-\beta m v^2/2 - \beta V(q)} \xi_{SS}(q, v)}{\int e^{-\beta m v^2/2 - \beta m \omega_A^2 (q - q_A)^2} dq dv} = \frac{m\omega_A}{2\pi k_B T} e^{-\beta m v^2/2 - \beta V(q)} \xi_{SS}(q, v) \quad (16.1.11)$$

Additionally, the Klein-Kramers equation that gave $\rho_{SS}(q, v)$ is a continuity equation, so an equivalent rate will be obtained regardless of the dividing surface as long as it separates the reactant and product states. The calculation is most easily done for the dividing surface $q = 0$.

$$k_K = \int_{-\infty}^{\infty} v\rho_{SS}(0, v)dv \tag{16.1.12}$$

where k_K is the Kramers rate constant. The flux integral can be simplified by using $vexp[-mv^2/(2k_BT)] = -(k_BT/m)\partial exp[-mv^2/(2k_BT)]/\partial v$ and then integrating by parts. The result of the integration is the Kramers rate constant

$$k_K = \frac{\gamma}{\omega_\ddagger}\left(\sqrt{\frac{1}{4} + \frac{\omega_\ddagger^2}{\gamma^2}} - \frac{1}{2}\right)\frac{\omega_A}{2\pi}exp\left[-\beta V_\ddagger\right]$$

Recall that classical TST in one dimension gave $k_{TST} = (\omega_A/2\pi)exp(-V_\ddagger/k_BT)$. Thus the Kramers theory rate is $k_K = \kappa_K k_{TST}$ where κ_K is the Kramers transmission coefficient [1]

$$\kappa_K = \frac{\gamma}{\omega_\ddagger}\left(\sqrt{\frac{1}{4} + \frac{\omega_\ddagger^2}{\gamma^2}} - \frac{1}{2}\right) \tag{16.1.13}$$

Figure 16.1.5 shows κ_K as a function of $\gamma/\omega_\ddagger$. If we studied a bimolecular reaction, then the reactant partition function would change so as to equally modify $\rho_{SS}(x, v)$ and the TST rate constant. Therefore the transmission coefficient would still be that given in equation (16.1.13) [7].

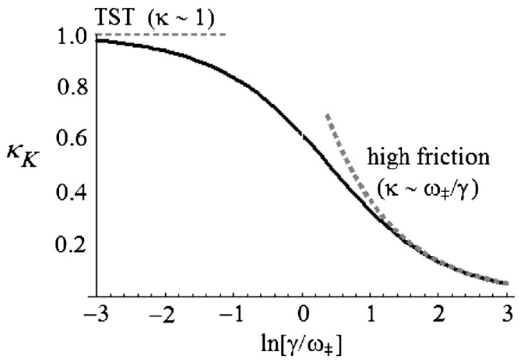

Figure 16.1.5: The transmission coefficient from Kramers theory for intermediate friction and assuming a parabolic barrier. At low friction the transmission coefficient of equation (16.1.13) becomes unity and at high friction it becomes inversely proportional to the friction.

At high friction, the dynamics along the reaction coordinate begin to resemble diffusion along the reaction coordinate as shown in Figure 16.1.6 and k_K becomes the mean first passage rate:

$$k_{MFP} = \frac{\omega_\ddagger}{\gamma}k_{TST} \tag{16.1.14}$$

The Kramers transmission coefficient does not explicitly depend on temperature, but strong temperature dependence may enter through the friction. γ is related to diffusivity along the reaction coordinate via the Einstein relation: $D = k_B T/m\gamma$. Based on theories of diffusion in liquids and glasses, γ should increase approximately in proportion to the viscosity. For solute precipitate nucleation in solids, γ is inversely proportional to the rate of solute diffusion - a process that typically occurs by vacancy hopping and/or other activated processes. Thus both viscosity and solid-state diffusivities can lead to a strong, even Arrhenius-like, temperature dependence *within the prefactor* of the high friction Kramers rate constant. See Chapter 18 for more details on these effects.

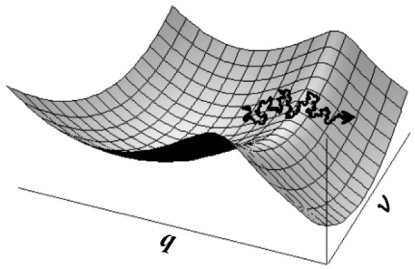

Figure 16.1.6: When $\gamma \gg \omega_{\ddagger}$ the dynamics resemble diffusion over the barrier top, and the Kramers transmission coefficient becomes $\omega_{\ddagger}/\gamma$.

This section has shown that Kramers theory encompasses regimes from the direct dynamics of TST to the overdamped dynamics of processes like protein folding and nucleation. As the next section shows, Kramers theory can also qualitatively describe dynamical effects of slow energy relaxation at low friction.

16.2 Low friction: the energy diffusion limit

At low friction, the transmission coefficient in equation (16.1.13) approaches unity, suggesting that the Kramers rate constant should become that of TST. However, the validity of the TST limit at low friction depends on the nature of the energy landscape. If motion along the reaction coordinate can continue indefinitely in the forward and backward directions, as in a bimolecular reaction, then the low friction limit of Kramers theory does reduce to TST [7]. Reactive trajectory studies for some bimolecular reactions in the gas phase confirm that TST is essentially correct [23], but significant crossing is observed for reactions with highly curved paths [24,25]. Several other scenarios can also cause recrossing, even in the limit of low friction.

Chapter 9 discussed non-TST rate expressions for unimolecular reactions in low pressure gases where activation (and also deactivation) occurs by strong but infrequent collisions with other gas molecules. Kramers [1] instead models the effects of a small steady friction that limits the rate at which trajectories can acquire (and dissipate) activation energy. Trajectories in this weak friction limit oscillate, or "orbit", the reactant well many times before they can appreciably

change their energy level. Although Kramers' weak steady Langevin friction differs from the strong, infrequent, and prolonged collisions that occur in real gases, the model of Kramers qualitatively preserves the expected time scale hierarchy for weak coupling:

$$\omega_A^{-1} \ll \gamma^{-1} \ll k^{-1}$$

These time scales are the vibrational period in the reactant well, the time for vibrational energy dissipation (in lieu of rare collisions), and the escape time. Reactive trajectories for such a system will qualitatively resemble those shown in Figure 16.2.1 Note that the previous section envisioned $V(q)$ as a PMF or a free energy profile because the intermediate to high friction limit is most appropriate for processes in condensed phases. In the low friction limit, we envision $V(q)$ in the Langevin equation as the potential energy profile for a degree of freedom that is only weakly coupled to the other modes.

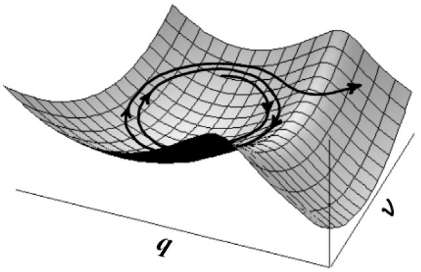

Figure 16.2.1: When $\gamma \ll \omega_A$ trajectories can orbit the reactant basin many times before dissipating energy on the order $k_B T$. This energy diffusion limited regime also lowers the transmission coefficient.

For low friction dynamics, the (q, v) coordinates are not ideal. Both q and v will oscillate wildly each time the system nearly acquires the transition state energy. Energy or action variables are more convenient because the rapid phase oscillations can be averaged out leaving the slowly varying energy or action variables [1,22]. Again we begin with an inertial Langevin equation, but now we multiply all terms by the velocity.

$$mv\dot{v} + v\frac{\partial V}{\partial q} = -m\gamma v^2 + vR(t) \tag{16.2.1}$$

If the total energy is $E = mv^2/2 + V(q)$, then the left hand side of equation (16.2.1) is dE/dt. Averaging over an oscillation period for a perfectly harmonic reactant well gives

$$\frac{dE}{dt} = -\gamma E + \overline{vR(t)}$$

The period-averaged random noise term continues to provide random kicks, but with an altered variance. Beyond this point the derivation is not easy. The Langevin equation is ultimately converted into a Smoluchowski equation for $\rho(E, t)$. The derivation requires a relationship

between the classical action and the energy: $dE/dS = \omega(E)$ [26]. We skip all of the details [27], and go straight to the energy diffusion Smoluchowski equation

$$\frac{\partial \rho}{\partial t} = \frac{\partial}{\partial E}\left\{\gamma S(E)\left(1 + k_B T \frac{\partial}{\partial E}\right)\Omega(E)^{-1}\rho\right\} \tag{16.2.2}$$

where $\Omega(E)$ is the density of states in the reactant well at energy E. The quantity $\gamma S(E)$ is the rate of energy diffusion into and out of the reaction coordinate.

We again seek a non-equilibrium steady-state solution to equation (16.2.2). In the energy diffusion limit, trajectories escape to the product state as soon as they acquire the necessary activation energy. Note the difference between Kramers and RRKM theory here. RRKM theory explicitly considers all modes of the reactant and their total energy. Upon sudden activation to a total energy that exceeds the threshold, the RRKM theory predicts a random waiting time for sufficient energy to become focused into the reaction coordinate. The low friction Kramers model explicitly considers only one degree of freedom. The waiting time in the Kramers model is for threshold activation of the one explicitly modeled reaction coordinate, and the reaction then promptly occurs. The low friction Kramers model therefore invokes the boundary condition

$$\rho_{SS}(V_\ddagger) = 0 \tag{16.2.3}$$

Trajectories that escape are replaced at the bottom of the reactant well to maintain a steady-state distribution. A calculation similar to the mean first passage time calculation for the high friction limit gives the energy dissipation limited (EDL) rate

$$k_{EDL}^{-1} = \beta \int_0^{V_\ddagger} dE\, \Omega(E) exp\left(-\beta E\right) \int_E^{V_\ddagger} \frac{dE'}{\gamma S(E')} exp[+\beta E']$$

The integral over E' primarily contributes when E' reaches values near $V_\ddagger$. The integral over E primarily contributes near the reactant minimum. An approximate evaluation of the integrals gives

$$k_{EDL} \approx \beta \gamma S(V_\ddagger) \frac{\omega_A}{2\pi} exp[-\beta V_\ddagger] \tag{16.2.4}$$

Normalizing by the TST rate, the energy diffusion limited transmission coefficient is

$$\kappa_{EDL} \approx \beta \gamma S(V_\ddagger) \tag{16.2.5}$$

Equation (16.2.5) says that the transmission coefficient is proportional to the action integral over the reactant well at the transition state energy $S(V_\ddagger) \approx V^\ddagger/\omega_A$. Qualitatively, the number of recrossings is the ratio of the time to dissipate $k_B T$ of energy and the vibrational period of the

stable well. As friction γ gets weaker, the time for dissipation grows, the number of recrossings grows, and the transmission coefficient goes down. Thus for unimolecular reactions, Kramers theory predicts a transmission coefficient that increases for low friction and then decreases for high friction. This result, shown in Figure 16.2.2, is the Kramers turnover.

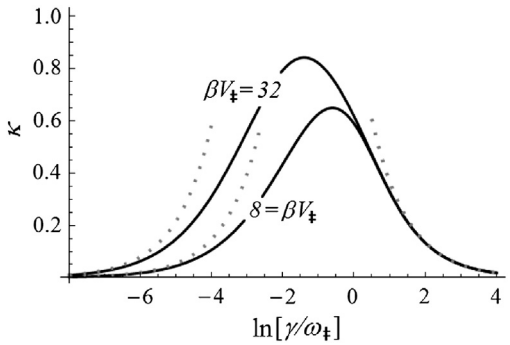

Figure 16.2.2: For purposes of illustration, suppose that the reactant well is harmonic and that $\omega_A = \omega_\ddagger$. The solid curves show the Melnikov-Meshkov transmission coefficient (κ_{MM}) for different values of $\gamma/\omega_\ddagger$ and $\beta V\ddagger$. The rightmost dotted curve shows the overdamped asymptotic transmission coefficient (κ_{MFP}). The dotted curves on the left show Kramers asymptotic low friction transmission coefficient (κ_{EDL}). Note that the low friction transmission coefficient depends on the barrier height but the high friction transmission coefficient does not.

Note that Kramers did not actually solve for the escape rate in the turnover friction regime. Mel'nikov and Meshkov [27,28] and Pollak et al. [29] developed the connection formulas that bridge the low and high friction regimes. Their routes to the connection formulas differ, but both consider the distribution of energy losses for trajectories that orbit the reactant basin at the barrier energy. Their common result is a Gaussian transition probability for the energy E_2 after one orbit beginning at energy E_1.

$$p(E_2|E_1) = (4\pi k_B T \gamma S_\ddagger)^{-1/2} exp\left[-\frac{(E_2 - E_1 + \gamma S_\ddagger)^2}{4k_B T \gamma S_\ddagger}\right]$$

In accordance with intuition, orbits started at $V_\ddagger$ tend to dissipate energy because $\gamma S_\ddagger > 0$. Mel'nikov and Meshkov used the energy transition probabilities to derive a transmission coefficient that bridges the high and low friction limits [28]

$$\kappa_{MM} = \frac{\gamma}{\omega_\ddagger}\left(\sqrt{\frac{1}{4} + \frac{\omega_\ddagger^2}{\gamma^2}} - \frac{1}{2}\right) exp\left\{\frac{1}{\pi}\int_0^\infty d\varsigma \frac{ln\left[1 - exp\left(\beta\gamma S(V_\ddagger)(\varsigma^2 + 1/4)\right)\right]}{\varsigma^2 + 1/4}\right\} \tag{16.2.6}$$

Mel'nikov and Meshkov also found that trajectories crossing the transition state have non-equilibrium velocity distributions. The average kinetic energy along q at the transition state increases from zero in the low friction limit to the equipartition value (i.e. to equilibrium) in the high friction limit [27]. The non-equilibrium distribution of kinetic energy at $q_{\ddagger}$ is also evident in Figure 16.1.4.

Because of the boundary condition in equation (16.2.3), the average kinetic energy (along the reaction coordinate) of trajectories as they cross the saddle region must approach zero as γ approaches zero. This finding stands in stark contrast to the perfectly equilibrium distribution of the velocities for the overdamped regime. Recall that reactive flux calculations use as initial conditions on the dividing surface an equilibrium velocity distribution, regardless of the friction and/or coupling strength [30,31]. The energy diffusion limit of Kramers theory pertains to a rather unrealistic model, but nevertheless this inconsistency with the reactive flux formalism might seem troubling. The apparent inconsistency can be resolved by considering the separate contributions [32] of the κ^+ (initially positive flux) and κ^- (initially negative flux) to κ as friction approaches zero for escape from a single well like that shown in Figure 16.2.1. Also revisit section 13.2 which explains that the transmission coefficient can be interpreted as the effects of recrossing for an ensemble of equilibrium transition states, or equivalently as a correction for non-equilibrium effects.

16.3 Insights and limitations

As a computational tool, Kramers theory is only occasionally useful – usually in analyses of simple models for which its assumptions are true by construction. However, Kramers theory was a conceptual breakthrough because it provides one unified framework for understanding how dynamics influence reaction rates. The key lessons from Kramers theory include:

A spatial diffusion limit: At high friction the rate decreases as γ^{-1} and approaches Pontryagin's [2] rate expression for diffusion over a barrier in the high friction limit (see Chapter 18).

An energy diffusion limit: At extremely low friction, escape from a potential well becomes limited by slow energy influx and dissipation. The transmission coefficient for these processes increases in proportion to the friction and the action per orbit, $\gamma S(E_{\ddagger})$ [1]. See Hanggi [26] and Mel'nikov [27] for an analysis of related effects on the kinetics of interconversion between two potential wells (e.g. in isomerization).

A turnover region: The transmission coefficient reaches a maximum for moderate friction. Transmission coefficients near the turnover are less than but comparable to unity [26,27].

There are many pitfalls to avoid in using Kramers theory and in interpreting its results. First, we should not expect an energy diffusion limit for atom exchange reactions or S_N2 reactions in

the gas phase. Although such bimolecular reaction trajectories may proceed ballistically with little friction, the reactants and products can travel indefinitely backward and forward along the reaction coordinate. Simulation evidence [23–25,33,34] suggests that when barrier recrossing occurs in these reactions it arises for other reasons, e.g. from pathways that curve sharply near the saddle point.

There are quantitative problems with the energy diffusion limit even for reactions that do involve bound wells where slow energy transfer can be limiting. Kramers' weak, steady Langevin friction model is not accurate for energy transfer by strong and sudden, but infrequent collisions with other molecules. In fact, Kramers' energy diffusion limit is valid only when the energy transfer per orbit is less than $k_B T$ [26,27]. Several investigators have developed alternative theories for the weak coupling limit [4,35,36].

Kramers theory describes a one-dimensional reaction coordinate coupled to a bath. Especially for intermediate friction, the bath is frequently envisioned to be the solvent. Technically, the bath must also include intramolecular modes other than the reaction coordinate, and therefore the friction includes "internal friction" from coupling to these modes [14,16,37]. Especially for reactions involving large molecules like proteins, intramolecular friction can be more important than friction from the surrounding solvent. Thus models and predictions where friction exclusively stems from solvent viscosity should be used with caution.

In the Kramers model, friction is a constant at every point along the reaction coordinate, but intramolecular contributions to the friction are often coordinate dependent [38–41]. These studies suggest that dynamics along different modes at a saddle point may be separable, but farther along the pathway the coupling (friction) may become large and help to quench reactive trajectories.

Kramers theory assumes a delta-correlated friction and random forces, i.e. a bath that responds infinitely fast. For typical bond-breaking/bond-making reaction in solution, the barrier crossing time is $\omega_{\ddagger}^{-1} \sim 100$ fs. A bath of internal modes and solvent molecules typically includes a multitude of slower vibrational frequencies and librational motions that cannot adiabatically equilibrate to such rapid changes in the reaction coordinate. Therefore the Kramers model, in which the bath responds the same way regardless of the dynamical history, cannot be correct for reactions that break/make bonds. Grote-Hynes theory (see Chapter 17) uses a non-Markovian friction and random forces to provide a more accurate description of chemical reaction dynamics in condensed phases [7].

In the high friction (overdamped) limit, the barrier crossing time becomes much longer than the bath relaxation time, $\gamma/\omega_{\ddagger} \gg 1$. As examples, protein folding [19,42–44] electron transfer [45], and nucleation [46,47] are often modeled as overdamped processes. Each of these processes involve concerted motions of hundreds or thousands of atoms, and in some cases the barrier

crossing times can be nanoseconds. With so much time atop the barrier, faster motions (both solvent and internal non-reaction coordinates) will remain quasi-equilibrated throughout the barrier crossing event. The entire rate calculation reduces to a mean first passage time involving only a diffusion along the reaction coordinate and a free energy barrier. This high friction limit is where quantitative results from Kramers theory are most reliable. However, one must be wary of reaction coordinate error. Even in the limit of perfectly diffusive dynamics, choosing an incorrect reaction coordinate renders the one-dimensional description of Kramers theory inaccurate [17,48]. More will be said about this problem in Chapters 18 and 20.

Exercises

1. Nondimensionalize the inertial Langevin and Klein-Kramers equations using the rescaled variables: $\tau = \gamma t$, $\underline{v} = v\sqrt{m/k_BT}$, and $\underline{q} = \gamma q\sqrt{m/k_BT}$. After nondimensionalization, what happens to the variance of random noise $\langle \Re(0)\Re(t)\rangle = (?)\delta[t]$ in the inertial Langevin equation?
2. Write a code to compute the reactive flux correlation function from inertial Langevin trajectories on the potential $\beta V(q) = \beta V_{\ddagger}(1 - 3q^2 - 2q^3)$.
   (a) Separately compute the κ^+ and κ^- contributions to κ at γ = 0.01, 0.1, 1.0, 10.0, and 100.0.
   (b) Explain the observed trends in the κ^+ and κ^- contributions to κ.
   (c) Compare your numerical results to the Kramers turnover expression from Mel'nikov and Mesh'kov.
3. Begin with an inertial Langevin equation and compute the rate of crossing over a square topped barrier of size ΔF and width L. Assume a perfectly absorbing boundary condition at the right edge of the barrier and equilibrium for states beyond the left edge of the barrier. Compare your result to the transition state theory rate.
4. Compute the transmission coefficient for crossing over a sharp cusp shaped barrier. Hint: this problem is outlined in Kramers' 1940 paper. Complete the details.
5. Read Shoup and Szabo, Biophys. J. 40, 33 (1982). Describe in detail the relationship between the Debye model for diffusion control and the overdamped limit of Kramers theory.
6. Read Vekilov, Cryst. Growth & Design 7, 2796–2810 (2007) on crystal growth kinetics. Derive the mass dependences for an Eyring-like (inertial) attachment dynamics and a Kramers/Debye-like diffusional attachment. Check your predictions against those of Vekilov and the evidence cited therein.

References

[1] H.A. Kramers, Physica A 7 (1940) 284–304.
[2] L.S. Pontryagin, A.A. Andronov, A.A. Vitt, Zh. Eksp. Teor. Fiz. 3 (1933) 165–180.

[3] V. Agarwal, B. Peters, Adv. Chem. Phys. 155 (2014) 97–160.
[4] J.L. Skinner, P.G. Wolynes, J. Chem. Phys. 69 (1978) 2143.
[5] M. Jacob, M. Geeves, G. Holtermann, F.X. Schmid, Nat. Struct. Biol. 6 (1999) 923–926.
[6] R.I. Masel, Chemical Kinetics and Catalysis, Wiley, New York, 2001.
[7] J.T. Hynes, Annu. Rev. Phys. Chem. 36 (1985) 573–597.
[8] P.G. Wolynes, in: D. Stein (Ed.), Complex Systems, in: SFI Studies in the Sciences of Complexity, Addison-Wesley, Longman, 1989, pp. 355–387.
[9] R.F. Grote, J.T. Hynes, J. Chem. Phys. 73 (1980) 2715–2732.
[10] J.T. Hynes, in: O. Tapia, J. Bertran (Eds.), Solvent Effects and Chemical Reactivity, Kluwer, Amsterdam, 1996, pp. 231–258.
[11] E. Pollak, J. Chem. Phys. 85 (1986) 865–867.
[12] J.S. Langer, Ann. Phys. 54 (1969) 258–275.
[13] A.M. Berezhkovskii, E. Pollak, V. Yu, J. Chem. Phys. 97 (1992) 2422–2437.
[14] S.J. Hagen, Curr. Protein Pept. Sci. 999 (2010) 1–11.
[15] J.M. Anna, K.J. Kubarych, J. Chem. Phys. 133 (2010) 174506.
[16] J.J. Portman, S. Takada, P.G. Wolynes, J. Chem. Phys. 114 (2001) 5082.
[17] A. Berezhkovskii, A. Szabo, J. Chem. Phys. 122 (2005) 14503.
[18] C.D. Snow, Y.M. Rhee, V.S. Pande, Biophys. J. 91 (2006) 14–24.
[19] S.V. Krivov, M. Karplus, Proc. Natl. Acad. Sci. USA 105 (2008) 13841–13846.
[20] B. Peters, Chem. Phys. Lett. 554 (2012) 248–253.
[21] W.A. Coffey, Y.P. Kalmykov, J.T. Waldron, The Langevin Equation, World Scientific, Singapore, 2004.
[22] A. Nitzan, Dynamics in Condensed Phases: Relaxation, Transfer, and Reactions in Condensed Molecular Systems, Oxford University Press, Oxford, 2006.
[23] H. Hu, M.N. Kobrak, C. Xu, S. Hammes-Schiffer, J. Phys. Chem. A 104 (2000) 8058–8066.
[24] Y.J. Cho, S.R. Vande Linde, L. Zhu, W.L. Hase, J. Chem. Phys. 96 (1992) 8275.
[25] W.L. Hase, Science 266 (1994) 998–1002.
[26] P. Hanggi, J. Stat. Phys. 42 (1986) 105–148.
[27] V.I. Mel'nikov, Phys. Rep. 209 (1991) 1–71.
[28] V.I. Mel'nikov, S.V. Meshkov, J. Chem. Phys. 85 (1986) 1018.
[29] E. Pollak, H. Grabert, P. Hanggi, J. Chem. Phys. 91 (1989) 4073–4087.
[30] D. Chandler, J. Chem. Phys. 68 (1978) 2959–2970.
[31] J.E. Straub, M. Borkovec, B.J. Berne, J. Chem. Phys. 84 (1986) 1788–1794.
[32] R.A. Kuharski, D. Chandler, J.A. Montgomery, F. Rabii, S.J. Singer, J. Phys. Chem. 92 (1988) 3261–3267.
[33] T. Su, H. Wang, W.L. Hase, J. Phys. Chem. A 102 (1998) 9819–9828.
[34] L. Sun, W.L. Hase, K. Song, J. Am. Chem. Soc. 123 (2001) 5753–5756.
[35] E.W. Montroll, K.E. Shuler, Adv. Chem. Phys. 1 (1958) 361–399.
[36] J. Troe, Annu. Rev. Phys. Chem. 29 (1978) 223–250.
[37] A. Soranno, B. Buchli, D. Nettels, R.R. Cheng, S. Muller-Spath, S.H. Pfeil, A. Hoffmann, E.A. Lipman, D.E. Makarov, B. Shuler, Proc. Natl. Acad. Sci. USA 109 (2012) 17800–17806.
[38] B. Carmeli, A. Nitzan, Chem. Phys. Lett. 102 (1983) 517–522.
[39] G.R. Haynes, G.A. Voth, J. Chem. Phys. 103 (1995) 10176.
[40] H. Wang, W.L. Hase, Chem. Phys. 212 (1996) 247–258.
[41] B. Peters, A.T. Bell, A. Chakraborty, J. Chem. Phys. 121 (2004) 4453–4460.
[42] J.N. Onuchic, Z. Luthey-Schulten, P.G. Wolynes, Annu. Rev. Phys. Chem. 48 (1997) 545–600.
[43] D.J. Bicout, A. Szabo, Protein Sci. 9 (2000) 452–465.
[44] S. Beccara, T. Skrbic, R. Covino, P. Faccioli, Proc. Natl. Acad. Sci. USA 109 (2012) 2330–2335.
[45] D.F. Calef, P.G. Wolynes, J. Phys. Chem. 87 (1983) 3387–3400.
[46] D. Kashchiev, Nucleation: Basic Theory with Applications, Butterworth-Heinemann, Oxford, 2000.
[47] K.F. Kelton, A.L. Greer, Nucleation in Condensed Matter: Applications in Materials and Biology, Elsevier, Amsterdam, 2010.
[48] Y.M. Rhee, V.S. Pande, J. Phys. Chem. B 109 (2005) 6780–6786.